Age-Critical Long Erasure Coding-CCSDS File Delivery Protocol for Dual-Hop S-IoT

Jianhao Huang, Jian Jiao, *Senior Member, IEEE*, Ye Wang, *Member, IEEE*, Shaohua Wu, *Member, IEEE*, Rongxing Lu, *Fellow, IEEE*, and Qinyu Zhang, *Senior Member, IEEE*

***Abstract*—The upcoming Satellite Internet of Things (S-IoT) can provide status updates relaying for ground user equipment (UE). However, the S-IoT cannot utilize the conventional hybrid automatic retransmission request (HARQ) for reliable transmission due to the high bit error rate (BER) and long propagation latency. The consultative committee for space data systems (CCSDSs) has proposed the CCSDS file delivery protocol (CFDP) to relieve the long propagation latency, and the CFDP utilizes retransmission to guarantee the reliability. In this article, we propose two age-critical long erasure coding-CFDP (LEC-CFDP) schemes to realize dual-hop timely status updates in S-IoT via a relay satellite over shadowed Rician (SR) fading channel, where the satellite and destination can select the deferred or asynchronous mode to adjust the number of inserted long erasure codes (LECs) packets, called D-LEC CFDP and A-LEC CFDP, respectively. Furthermore, the satellite can select half-duplex or full-duplex relay mode, i.e., LEC-h CFDP or LEC-f CFDP to forward packets to the destination. We derive a closed-form expression for the Peak Age of Information (PAoI) and an approximation expression for the expected end-to-end delay for the D-LEC-f CFDP scheme. Moreover, we propose an A-LEC-f CFDP scheme to further improve the PAoI, and model it as a partially observable Markov decision process (POMDP) problem, which can be solved by a low-complexity point-based informed bound (PIB) algorithm. Simulation results verify the accuracy of the theoretical derivations and illustrate that the A-LEC-f CFDP scheme can achieve lower end-to-end delay and PAoI in comparison with the existing schemes.**

***Index Terms*—Age of Information (AoI), consultative committee for space data system (CCSDS) file delivery protocol, long erasure coding, partially observable Markov decision process (POMDP), Satellite Internet of Things (S-IoT).**

Manuscript received 11 December 2022; revised 24 February 2023; accepted 26 April 2023. Date of publication 9 May 2023; date of current version 25 September 2023. This work was supported in part by the National Natural Sciences Foundation of China (NSFC) under Grant 62071141, Grant 61871147, Grant 61831008, and Grant 62027802; in part by the Shenzhen Science and Technology Program under Grant JSGG20220831110801003 and Grant GXWD20201230155427003-20200822165138001; and in part by the Major Key Project of PCL Department of Broadband Communication. *(Corresponding authors: Jian Jiao; Qinyu Zhang.)*

Jianhao Huang, Jian Jiao, Shaohua Wu, and Qinyu Zhang are with the Guangdong Provincial Key Laboratory of Aerospace Communication and Networking Technology, Harbin Institute of Technology (Shenzhen), Shenzhen 518055, China, and also with the Peng Cheng Laboratory, Shenzhen 518055, China (e-mail: 22S152095@stu.hit.edu.cn; jiaojian@hit.edu.cn; hitwush@hit.edu.cn; zqy@hit.edu.cn).

Ye Wang is with Peng Cheng Laboratory, Shenzhen 518055, China (e-mail: wangy02@pcl.ac.cn).

Rongxing Lu is with the Faculty of Computer Science, University of New Brunswick, Fredericton, NB E3B 5A3, Canada (e-mail: rlu1@unb.ca).

Digital Object Identifier 10.1109/JIOT.2023.3274519

I. Introduction

With the commercial applications of the fifth-generation (5G) mobile communication and the in-depth research of the sixth generation (6G), the Satellite Internet of Things (S-IoT), which can provide seamless communication coverage and instant response for a wide geographical area and extreme terrain, has attracted considerable attention [1]. Moreover, with the upcoming applications for S-IoT, higher information freshness becomes an urgent need for many emerging timeliness applications [2], such as environmental monitoring, smart grid, and voyage navigation [3]. Consider the information freshness is a destination-centric measurement that only focuses on the latest successfully received status update, which implies that traditional communication indicators, such as delay, cannot fully characterize it [4]. Therefore, to evaluate information freshness, a timeliness metric named Age of Information (AoI) is introduced in this article, which is defined as the time elapsed since the most recently received status update [5].

Moreover, low Earth orbits (LEOs) high-throughput satellite (HTS) can collect the status updates and forward them over the inter- or intrasatellite links to the ground station [6], [7]. However, the satellite–territory link (STL) have nontrivial propagation delay and high bit error rate (BER), which would lead to additional retransmission rounds and larger propagation delay, and severely deteriorating the freshness of the received status updates [8], [9], [10]. Note that the consultative committee for space data systems (CCSDSs) has proposed the CCSDS file delivery protocol (CFDP), which can relieve the long propagation latency and poor timeliness in space communications by reducing the feedback rounds [11]. In addition, two reliable transmission modes are proposed in CFDP, named the deferred and asynchronous modes, where the receiver feeds back the acknowledgment (ACK) or non-ACK (NAK) after receiving all the packets of status update in the deferred mode, and sends the NAK according to the predetermined trigger in the asynchronous mode. Yang et al. [12] proposed a CFDP-based two-hop relaying protocol (CTRP), where the relay satellite immediately forwards the received protocol data unit (PDU) packets in a full-duplex mode, which can significantly reduce the end-to-end delay. Furthermore, CCSDS released the long erasure codes (LECs) specification [13] to perform a packet-level LEC at the transport layer, and the receiver could recover the lost PDUs by utilizing the LEC PDU packets. Therefore, to fulfil the requirement of reliable transmission and avoid retransmission to achieve lower AoI, we propose two

age-critical long erasure coding-CFDP (LEC-CFDP) schemes to realize dual-hop timely status updates in S-IoT.

A. Related Works

AoI is a time-sensitive performance metric, which is different from the end-to-end delay in wireless communications [14]. Jiao et al. [15] studied the Average AoI (AAoI) of a two-hop system with packet arrivals only at the first node and zero-waiting policy at the second node. The analysis and optimization of Peak AoI (PAoI) is studied for the two-hop tandem exponential queues with multiple sources in [16]. Moradian and Dadlani [17] analyzed and optimized the AoI with static link scheduling policies through the Markovian jump linear systems in two wireless relay networks. However, their works do not take the reliable transmission into account, which are not suitable for satellite communication. Moreover, there are multiple packets that may be generated at the same time in a status update, and AAoI cannot exactly characterize the freshness in this case. Since the PAoI can capture the recovery of the last packet in each status update transmission [18], it is introduced into our scheme to measure the freshness.

Nevertheless, the bit-level forward error correction (FEC) approaching the Shannon limit still cannot guarantee the reliable transmission due to the high BER in STL [19], [20]. Cohen et al. [21] proved that the LEC in the transport layer can effectively alleviate the packet lost in the physical layer to reduce the retransmission rounds in space communication. The random linear network coding (RLNC) is an excellent LEC scheme to provide high-efficiency transmission in downlink satellite-to-ground scenario [22], where the original n information packets can be recovered with a large probability by successfully receiving n NC packets, thus completing the status update. In [23], the RLNC scheme has been proved that it can achieve lower delay and AoI than several classical hybrid automatic retransmission request (HARQ) schemes in S-IoT.

However, the satellite cannot know the precise channel status information (CSI) over the widely used shadowed Rician (SR) channel in satellite communications [24], [25]. Thus, the satellite is hard to select an appropriate number of LEC packets, which would lead extra delay and energy consumption to guarantee reliability. Note that the partially observable Markov decision process (POMDP) can model this unprecise CSI and minimum-AoI communication problems [10], [26], [28], Yao et al. [26] analyzed the transmission scheduling of a status update system without channel sensing, and apply POMDP to minimize the long-run AoI under the energy constraint. Ding et al. [27] investigated an end-to-end NC HARQ transmission scheme with delayed CSI through POMDP and making transmission decision to lower PAoI. In [28], POMDP is used to formulate the minimum-age scheduling problem in a wireless network, where the real-time AoIs of all sensors are unknown. Moreover, since POMDP is polynomial space hard to solve as it requires exponential computational complexity and memory, several algorithms such as point-based methods [29] have been proposed to solve it.

Therefore, to take both timeliness and reliability into consideration, we propose two age-critical LEC-CFDP schemes in the dual-hop S-IoT transmission scenario based on the deferred and asynchronous CFDP modes, which can adjust the LEC PDU packets insertion after or during the transmission of status update, respectively. Moreover, we propose two relay modes inspired by the CFDP and CTRP, and apply them to our proposal schemes. Then, according to the difference between uplink and downlink transmission, we formulate the dual-hop transmission as two appropriate POMDP models, respectively.

B. Contributions

The main contributions of this article can be summarized as follows.

1) We introduce a deferred-LEC CFDP (D-LEC CFDP) scheme for the dual-hop S-IoT transmission scenario, where the sender and relay satellite insert an LEC PDU after every $L-1$ information PDUs to accelerate the recovery of lost information PDUs, and L can be adjusted via the ACK/NAK after each transmission of status update. Moreover, we propose two D-LEC CFDP schemes based on two relay modes, named D-LEC CFDP with half-duplex relay mode (D-LEC-h CFDP) and D-LEC CFDP with full-duplex relay mode (D-LEC-f CFDP), respectively.
2) We analyze the D-LEC-f CFDP scheme, since it can lower the PAoI and expected end-to-end delay than that of the D-LEC-h CFDP scheme, when the channel at moderate and high signal-to-noise ratio (SNR) regions, while the latter can only achieve slightly better performance with lower complexity at low SNR. In addition, to yield the insight into the performance of the D-LEC-f CFDP, we derive a closed-form expression for PAoI and an approximate expression for the end-to-end expected delay by using the renewal process, which also provides a theoretical fundament to estimate the appropriate insert position of LEC PDU to guarantee the freshness.
3) We further propose an asynchronous LEC CFDP with full-duplex relay mode (A-LEC-f CFDP) scheme to improve the PAoI of D-LEC-f CFDP scheme at low SNR, where L can be adjusted via the ACK/NAK during the transmission of status update with a predetermined trigger at the receiver. Moreover, we introduce the POMDP to model the transmission and minimize the PAoI and end-to-end delay. Furthermore, we design a low-complexity optimization algorithm called point-based informed bound (PIB) to solve this POMDP problem. Finally, simulation results validate the accuracy of our theoretical derivations and show that the A-LEC-f CFDP scheme can outperform the D-LEC-f CFDP scheme and state-of-the-art scheme.

C. Outline

The remainder of this article is organized as follows. In Section II, we introduce the system model, the D-LEC CFDP dual-hop transmission schemes and the channel model. In

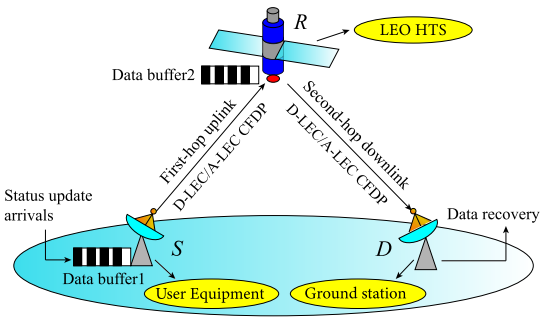

Fig. 1. Illustration of the dual-hop S-IoT transmission scenario.

Section III, we analyze the PAoI and expected end-to-end delay in the D-LEC-f CFDP scheme. In Section IV, we propose the A-LEC-f CFDP scheme based on POMDP, and solve it by a low-complexity PIB algorithm. Simulation results are presented in Section V. Finally, we conclude this article in Section VI.

II. System Model

We consider a dual-hop S-IoT transmission scheme as illustrated in Fig. 1, where a user equipment (UE) S collects status updates and transmits them to a relay satellite R, which is a LEO HTS and covers a wide remote area. Then, the received PDUs are forwarded by R to the ground station D as soon as possible. The channel from S to R and R to D are both modeled as the widely used SR fading channel [24], [25].

In the S-IoT dual-hop transmission scenario, we assume that there are n information PDUs and $\lceil n/(L-1) \rceil$ LEC PDUs in a status update, and these PDUs are temporarily buffered at S and then transmitted in order. Note that S can get the real-time CSI, while R only has delayed CSI because of the long STL propagation latency over time-varying SR fading channel. When these PDUs are relayed to R, R selects an appropriate relay mode and determines L to forward them to D as shown in Fig. 1. At the receiver side, if the ith information PDU is successfully received and all previous transmitted PDUs have been uploaded, it can be uploaded to the application layer. Otherwise, it is backlogged until the previous lost PDUs all be recovered by the later received LEC PDUs. Additionally, R and D are equipped with a single buffer with infinite capacity.

Consider the asymmetric link in satellite communications, we assume that the duration of 1.5 time slot equals the uplink transmission delay t_{s_1} for a 1-kB PDU specified by CFPD [11], while the downlink transmission delay t_{s_2} is one time slot for a PDU, and t_r denotes the propagation delay. Moreover, since the LEO HTS has much larger Doppler shift than GEO/MEO due to the high mobility, the method to handle it is one of the main issues that being studying in the Third Generation Partnership Project (3GPP), which is called the Doppler compensation [30], [31], [32]. We can first precompensate the Doppler shift roughly by exploiting the predictability of the satellite's movement [30]. After that, a refine precompensation of the oscillator offsets should be performed by utilizing a phase-locked loop (PLL) to track the reference tone [31]. Furthermore, Consider the bandwidth of

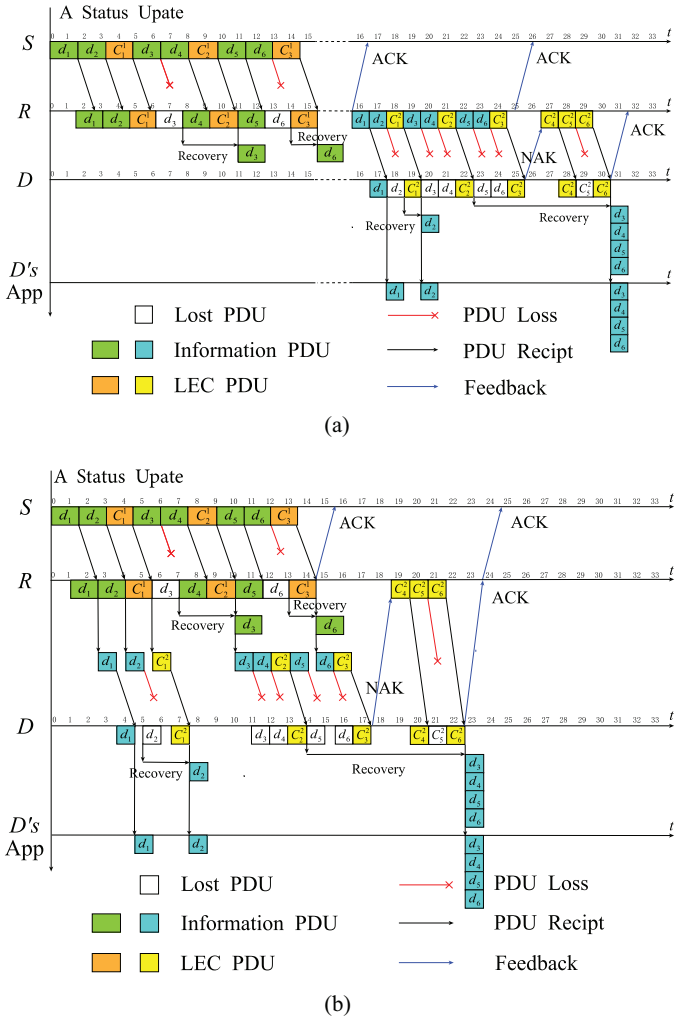

Fig. 2. Dual-hop illustration of our D-LEC CFDP scheme, where L_1 and L_2 are the LEC PDU inserted interval in the first and second hop, respectively. (a) D-LEC-h CFDP transmission scheme, where $n = 6$ and $L_1 = L_2 = 3$. (b) D-LEC-f CFDP transmission scheme, where $n = 6$ and $L_1 = L_2 = 3$.

HTS is about 800 MHz–2 GHz, a guard band that double than the Doppler shifts can be utilized to relieve the influence of Doppler shifts on the system [32].

As shown in Fig. 2, in our D-LEC CFDP scheme, each status update includes $\lceil n/(L-1) \rceil$ LEC PDUs generated via RLNC from a sufficiently large field to combat the erasures of information PDU, where an LEC PDU $C_j^k (j = 1, 2, \ldots, \lceil n/(L-1) \rceil, k = 1, 2)$ is encoded from all the preceding information PDUs $d_i (i = 1, 2, \ldots, (L-1)j)$ in the kth hop, and is periodically sent after the transmission of $L-1$ information PDUs [33]. Hence, the lost PDUs can be successfully recovered when the number of LEC PDUs collected by the receiver is equal to that of the lost information PDUs. Moreover, the precise SNR of CSI is estimated from the receiving signals at the receiver [34], and feeds back to the transmitter within 2–3 bits in the ACK or NAK at the end of receiving the last PDU, the transmitter adjusts L or retransmits according to the feedback [11], and the related notations are summarized in Table I.

TABLE I
RELEVANT NOTATION

notation	Definition
n	The number of information PDUs in a status update
B	The PDU size
L_k	The LEC interval in k-hop transmission
p_k	The block error rate in k-hop transmission
T	The feedback delay in the A-LEC CFDP scheme
t_r	The prorogation delay
t_{s_1}	The uplink transmission delay
t_{s_2}	The downlink transmission delay
D_i	The end-to-end delay of an information PDU d_i
D_q	The queueing time
D_f	The forwarding time
D_s	The service time
X_q	The number of LEC PDUs in q-th busy stage
B_q	The length of the first L-interval in q-th busy stage
X_m	The number of LEC PDUs in the largest X_q
X_a	The number of transmitted LEC PDUs in X_1 that failed to receive the first PDU
$Q^k(i)$	The queue length of d_i at k-th hop receiver
Q_m^k	The maximum queue length at k-th hop receiver
$\hat{N}_k$	The total number of PDUs in k-th hop transmission
T_{fe}^k	The feedback delay in k-th hop transmission
T_{re}^k	The retransmission time in k-th hop transmission

A. D-LEC CFDP Scheme and Relay Mode

In this section, we propose the D-LEC CFDP scheme with two relay modes in dual-hop S-IoT to satisfy higher freshness requirement. Since the basic idea of D-LEC CFDP scheme has been introduced above, we focus on two relay forward schemes, named the D-LEC-h CFDP transmission scheme as shown in Fig. 2(a), and the D-LEC-f CFDP transmission scheme as shown in Fig. 2(b).

In the D-LEC-h CFDP scheme, both R and D feed back ACK or NAK until receive all PDUs of the status update, and R would not forward any PDU until the first-hop transmission is completed at $t = 15$ as shown in Fig. 2(a). Then, R selects $L_2 = 3$ according to the last received CSI from D, and transmit PDUs as same as the first-hop transmission. Moreover, $L_2 = 3$ is not suitable for R due to the CSI is worse in the second hop, which means that D needs retransmission from R. Therefore, the HTS sends three LEC PDUs C_4^2, C_5^2, and C_6^2 according to the NAK at $t = 27$, and D utilizes them to recover four lost PDUs at $t = 30.5$. Finally, all information PDUs are uploaded to the application layer in order.

On the other hand, R would start transmission immediately when the first PDU could be sent in the D-LEC-f CFDP scheme, i.e., each successfully received or recovered PDU is immediately forwarded, if there is no more PDU with smaller sequence number than itself, such as d_1 and d_2. Otherwise, the PDUs are backlogged at the transport layer in R, i.e., d_4 recovered at $t = 8$ cannot be forwarded before d_3 is recovered by C_2^1 at $t = 10$. The transmission is finished at $t = 22.5$ in the D-LEC-f CFDP scheme, which means the D-LEC-f CFDP can achieve about 28% lower PAoI compared with D-LEC-h CFDP in the same channel condition, without considering the influence of self interference (SI) [35].

It is worth noting that unlike S, which can get real-time CSI and make correct decisions on L, R can only receive the delayed CSI. Therefore, when the CSI of R to D turns to bad, D always needs retransmission to recover the lost information PDUs, which evidently deteriorates the performance of expected end-to-end delay and PAoI. Thus, we design the A-LEC CFDP with full-duplex relay mode (A-LEC-f CFDP) to solve the problem.

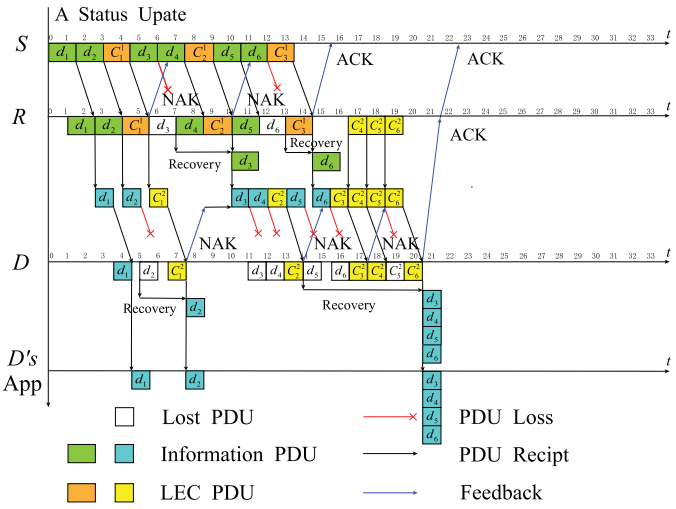

Fig. 3. Dual-hop illustration of a status update transmission in the A-LEC-f CFDP scheme, where $n = 6$ and $T = 3$.

B. A-LEC-f CFDP Scheme

We propose the A-LEC-f CFDP scheme to further improve the timeliness over SR fading channel in this section, where S or R can receive NAKs from R or D in each T time slots, and reselect an appropriate L according to the NAK to avoid retransmission. Next, we describe the example A-LEC-f CFDP scheme as shown in Fig. 3, where the channel condition is the same as that in Fig. 2.

In the first-hop transmission, it is identical to the D-LEC-f CFDP scheme since S can get the real-time CSI and make proper decision. But in the second-hop transmission, when d_3 and d_4 fail to be received at D, and the LEC PDU C_2^2 received at $t = 14$ cannot recover both d_3 and d_4. Thus, R reselects a new L_2 by the NAK received at $t = 15$ and immediately transmits three LEC PDUs. Thus, D utilizes them to recover the lost information PDUs at $t = 20.5$, and all PDUs can be uploaded at this time. Else if there are no new PDUs, and the receiver needs LEC PDUs to recover the lost PDUs, the sender would set $L = 1$, and calculate the number of LEC PDUs $n_L/(1 - P_e) + v_L (v_L \leq n - n_L)$ that needs to be transmitted, where n_L is the number of lost information PDU at that moment, P_e is the erasure probability and v_L is the redundancy of LEC PDUs.

To sum up, the A-LEC-f CFDP can reduce the consumption of time slots than the D-LEC-f CFDP in the same channel condition by sending extra NAKs. Note that an accurate block fading SR channel is modeled in the following, i.e., P_e is accurate enough to make R calculates the required number of LEC PDUs to recover all lost PDUs via the feedback CSI, there is no more than one retransmission round in our D-LEC CFDP and A-LEC CFDP schemes. Furthermore, to select a proper L with less frequency NAK feedback, we can design an

optimal POMDP transmission policy base on the SR channel as follows, and the details are given in Section IV.

C. Channel Model

The channel of S-IoT is modeled as the widely used SR fading channel in this article. We assume that the CSI remains constant during a status update, and randomly changes when the next status update comes. Thus, the probability density function (PDF) with instantaneous SNR r of SR fading channel can be written as follows [36]:

$$f(r) = \frac{1}{2b_0\gamma}\left(\frac{2b_0 m}{2b_0 m+\Omega}\right)^m \exp\left(-\frac{r}{2b_0\gamma}\right) \cdot {}_1F_1\left(m, 1, \frac{1}{2b_0\gamma}\left(\frac{\Omega}{2b_0 m+\Omega}\right)r\right) \tag{1}$$

where ${}_1F_1(.,.,.)$ is the confluent hypergeometric function, γ denotes the average value of SNR, Ω is the average power of LoS component, $2b_0$ is the average power of the multipath component, and $m(m \geq 0)$ is the parameter of channel fading severity.

The closed-form expression of BER with single antenna in SR fading channel is given in [23]. Moreover, to relieve the deep fading in SR channel, we introduce the multiple-input multiple-output (MIMO) system to improve BER [37]. Thus, the BER with MIMO system in SR fading channel can be derived as follows [26]:

$$P_e(\gamma) = \alpha^N \sum_{j=1}^{\max(M/4,1)} \xi_M \times \left(\frac{1}{\eta^N} - \frac{1}{\sqrt{2\pi}}\sum_{i=0}^{N-1}\frac{1}{i!}\frac{1}{2^{i-\upsilon}b_j^{2i}\eta^{N-i}\left(1+\eta/b_j^2\right)^{\upsilon}}\Gamma(\upsilon)\right) \tag{2}$$

where $N = N_r \times N_t$ is the diversity gain, depending on the number of receiving and transmitting antennas, $\alpha = [1/(2b_0\gamma)]([2b_0 m]/[2b_0 m+\Omega])^m$, $\eta = m/[(2b_0 m+\Omega)\gamma]$, $\upsilon = (2i+1)/2$, $\xi_m = \max(\log_2 M, 2)$, $b_k = \sin[(2k-1)\pi]/M$, and Γ is the Gamma function.

However, since the SR fading channel is quite volatile, the reliable transmission cannot be fully guaranteed in MIMO system [38]. Thus, we propose the A-LEC-i CFDP scheme to further reduce PAoI, where S or R can reselect a proper L via a POMDP optimization with feedback delay T and propagation delay t_r. The detailed analysis is introduced in Section IV.

III. Theoretical Analysis of D-LEC-f Scheme

In this section, we mainly analyze the expected end-to-end delay and PAoI of D-LEC-f CFDP scheme, since the derivation of these two indicators in the D-LEC-h CFDP scheme are similar to the successive transmissions of existing end-to-end schemes.

A. End-to-End Delay

Without loss of generality, we assume that S generates one update with $n(n > 0)$ information PDUs at $t = 0$. According to the transmission processes as shown in Fig. 2(b), the end-to-end delay D_i of an information PDU $d_i(i = 1, 2, \ldots, n)$ can be divided into four parts.

1) *Queueing Delay D_q:* The time elapses for the information PDU from its generation until its transmission at S.
2) *Forwarding Delay D_f:* The time elapses for the information PDU since it is received by R until forwarded to D.
3) *Service Delay D_s:* The time elapses for the information PDU since it is transmitted from R until it could be uploaded at D.
4) *Propagation Delay t_r:* The time elapses for the information PDU transmits from S to R, or R to D.

Hence, we have

$$D_i = D_q(i) + D_f(i) + D_s(i) + 2t_r. \tag{3}$$

Then, when d_i is to be transmitted, S has already sent $(i-1)$ information PDUs and $N_t = (\lceil i/[L_1 - 1]\rceil - 1)$ LEC PDUs. Therefore, $D_q(i)$ can be written as

$$D_q(i) = (N_t + i - 1)\cdot t_{s_1} \tag{4}$$

where t_s is the transmission delay and we assume that $t_{s_1} = 1.5t_{s_2} = 1.5t_r$. Therefore, the average queueing delay $(1/n)\sum_{i=1}^{n} D_q(i)$ can be further expressed as

$$\bar{D_q} = \frac{1}{n}\left(\sum_{j=1}^{n/(L_1-1)}(L_1-1)\cdot\left((j-1)\cdot L_1 + \frac{L_1-2}{2}\right)\right)\cdot t_{s_1} = \frac{(n-2)L_1+2}{2(L_1-1)}\cdot t_{s_1}. \tag{5}$$

Thus, by combining (3) and (5), the expected end-to-end delay $\bar{D} = (1/n)\sum_{i=1}^{n} D_i$ for the D-LEC-f CFDP scheme can be written as

$$\bar{D} = \frac{(n-2)L_1+2}{2(L_1-1)}\cdot t_{s_1} + 2t_r + \frac{1}{n}\sum_{i=1}^{n} D_f(i) + \frac{1}{n}\sum_{i=1}^{n} D_s(i). \tag{6}$$

We can find that the first and second terms of (6) are fixed in this scenario, while the third and fourth term depends on the channel status. Therefore, we introduce the concept of "busy/idle stage" in our transmission scheme for further analysis [33].

First, the "busy stage" refers to the time elapses since the transmission is suspended due to the lost information PDUs until that the received PDUs are all be recovered, e.g., as the time interval from $t = 11$ to $t = 22$ in the second-hop transmission as shown in Fig. 2(b). Then, we define X_q $(q = 1, 2, \ldots)$ as the number of transmitted LEC PDUs during the qth busy stage. We also define the "idle stage" as the period of sequential upload without waiting in the queue at the receiver. Note that X_q cannot accurately describe where the busy stage begins, because any information PDU can be the first lost PDU in an L PDUs transmission interval as shown in Fig. 2(b). Thus, we only use X_q to measure the length of the busy stage started from the second L-interval, i.e., $X_q \geq 1$, and denote B_q as the length of the first L-interval in the qth busy stage. Moreover, the idle stage is an exceptional case where there is only one L-interval in a busy stage. Therefore, X_q follows independent and

identically distributed (i.i.d.) due to the PDU lost is following i.i.d., and can be characterized by the probability distribution refers to [33]

$$P_{X_q}(x)=\begin{cases}(L\cdot p-p+1)(1-p)^{(L-1)}, & \text{for } x=1\\ \frac{L-1}{x}p^x(1-p)^{x(L-1)}\binom{(x-1)L}{x-1}, & \text{for } x>1\\ 0, & \text{otherwise}\end{cases} \tag{7}$$

where p is the block error rate (BLER), which can be calculated by the BER P_e and PDU size B as follows:

$$p=1-(1-P_e)^B. \tag{8}$$

Accordingly, it is easy to find the expectations that $E(X_q)=[(1-p)^L/1-L\cdot p]$ and $E(X_q^2)=E(X_q)+[L(L-1)p^2(1-p)^L/(1-L\cdot p)^3]$. Note that $E(X)$ is finite when $L\cdot p<1$, which indicates that the lost PDUs can be recovered by the previous transmitted LEC PDUs, i.e., it could avoid retransmission. Moreover, let p_k and L_k denote the BLER and inserted gap in the kth hop transmission, respectively. If the channel condition deteriorates and R dose not predict it because of the delayed CSI, it will lead to $L_2\cdot p_2\geq 1$. In this case, the received LEC PDUs cannot recover the lost information PDUs and the retransmission is necessary in the second-hop transmission as shown in Fig. 2. Thus, we provide the theoretical analysis for $L_k\cdot p_k<1$ and $L_k\cdot p_k\geq 1$ in our scheme in the following.

1) $L_k\cdot p_k<1$: Let $Q^k(i)$ denote the queue length of d_i at the kth hop receiver, which indicates the number of PDUs in a backlogged queue containing d_i, and Q_m^k denotes the maximum queue length at the kth hop receiver, and X_m denotes the number of transmitted LEC PDUs during the largest X_q. Thus, the expected of $(1/n)\sum_{i=1}^n Q^k(i)$ and Q_m^k in each hop can be expressed as follows:

$$\lim_{n\to\infty}\frac{1}{n}E\left(\sum_{i=1}^n Q^k(i)\right)=\frac{\left(E\left(X_q^2\right)-2E(X_q)+1\right)}{E(X_q)}\cdot(L_k-1)+\frac{E(X_q)\beta_1^k+\beta_2^k}{E(X_q)L_k} \tag{9}$$

and

$$E\left(Q_m^k\right)=(E(X_m)-1)L_k+\beta_3^k+E\left(T_{re}^k\right) \tag{10}$$

where β_1^k, β_2^k and β_3^k are three constants, which represent the impact of the first lost PDU on average queue length and maximum queue length in the kth hop transmission, respectively, and can be written as

$$\beta_1^k=\left(L_k-\frac{1}{p_k}\right)\left(1-(1-p_k)^{L_k-1}\right)+(L_k-1)(1-p_k)^{L_k-1} \tag{11}$$

and

$$\beta_2^k=\beta_1^k/L+\beta_1^k-L_k^2\left(1-(1-p_k)^{L_k-1}\right)+2/p_k^2+(1-p_k)^{L_k-1}\frac{(L_k-1)^2(1-p_k)-\left(L_k^2-2\right)+2/p_k}{p_k} \tag{12}$$

and

$$\beta_3^k=\frac{(p_k(L_k+1)-1)\left(1-(1-p_k)^{L_k-1}\right)}{p_k}+(L_k-1)(1-p_k)^{L_k-1}. \tag{13}$$

Their detailed derivation are given in Appendices A and B, respectively.

Note that the forwarding delay $D_f(i)$ of an information PDU d_i in the qth busy stage is affected both by X_q and the number of PDUs in all previous busy stage in R. In addition, in the transmission of a status update with n information PDUs, if d_M has the maximum queue length Q_m^1, all subsequent PDUs d_i $(n\geq i\geq M)$ after d_M are the same D_f, which can be expressed as $D_f=Q_m^1\cdot(t_{s_1}\cdot\eta_1+t_{s_2}\cdot\eta_2)$, where $\eta_1=[(L_1L_2-L_2)/(2L_1L_2-L_1-L_2)]$ and $\eta_2=[(L_1L_2-L_1)/(2L_1L_2-L_1-L_2)]$.

Therefore, we can assume that X_1 in R is the largest number in X_q to obtain a upper bound of average forwarding delay as $(1/n)\sum_{i=1}^n D_f(i)$. Furthermore, n information PDUs can be divided into $(n/[L-1])$ groups, and the probability of X_q starts from the ith information PDU in the $(j+1)$th Lth interval in R equals $P_R=p_1(1-p_1)^{j(L_1-1)+i-1}$. Meanwhile, we define $E(Q_m')$ as $E(Q_m^1)$ without considering the extra LEC PDUs, and the total number of lost information PDUs in R is $E(n_b)=E(Q^1)\cdot[(L_1-1)/L_1]$. Then, the expected of $(1/n)\sum_{i=1}^n D_f(i)$ can be expressed as (14), shown at the bottom of the page,

$$\lim_{n\to\infty}\frac{1}{n}E\left(\sum_{i=1}^n D_f(i)\right)\leq\sum_{j=0}^{(n-\lceil E(n_b)\rceil)/(L_1-1)}\sum_{i=1}^{L_1-1}P_R\cdot(n-i+1-jL_1)\cdot\left[E\left(Q_m'\right)\cdot\frac{t_{s_1}\cdot\eta_1+t_{s_2}\cdot\eta_2}{n}+\left(E\left(Q_m^1\right)-E\left(Q_m'\right)\right)\cdot\frac{t_{s_1}}{n}\right]+P_{re}\cdot E(n_b)\cdot\left[E\left(Q_m'\right)\cdot\frac{t_{s_1}\cdot\eta_1+t_{s_2}\cdot\eta_2}{n}+\left(E\left(Q_m^1\right)-E\left(Q_m'\right)\right)\cdot\frac{t_{s_1}}{n}\right] \tag{14}$$

$$\lim_{n\to\infty}\frac{1}{n}E\left(\sum_{i=1}^n D_s(i)\right)=\left[\frac{\left(E\left(X_q^2\right)-2E(X_q)+1\right)(L_2-1)}{2E(X_q)}+\frac{E(X_q)\beta_1^2+\beta_4}{E(X_q)L_2}\right]\cdot t_{s_2}+\sum_{j=\underline{X}}^{n/(L_2-1)}\Pr(X_q=j)\cdot(j\cdot\Pr(X_m=j)-1)L_1\cdot t_{s_1}\cdot\left(\frac{\beta_5+E(X_q)L_2-L_2}{E(X_q)L_2}\right) \tag{16}$$

where P_{re} denotes the probability that there is only X_1 in R as follows:

$$P_{re} = 1 - \sum_{j=0}^{(n-\lceil E(n_b)\rceil)/(L_1-1)} \sum_{i=1}^{L_1-1} P_{out}. \tag{15}$$

Similarly, the expected service delay D_s is not only affected by X_q in the ground station D but also affected by $D_f = Q_m^1 \cdot (t_{s_1} \cdot \eta_1 + t_{s_2} \cdot \eta_2)$ in R, which depends on the distribution of X_m as shown (16) at the bottom of the previous page. Let $\underline{X}$ denote the lower bound of X_m, and we can obtain the service delay without considering D_f through the derivation similar to (9), which is the first term in (16). Thus, the expected of $(1/n)\sum_{i=1}^{n} D_s(i)$ can be expressed in (16) at the top of this previous page, where β_4 and β_5 are constants and can be expressed as

$$\beta_4 = \beta_2^2 - \frac{\beta_1^2}{L_2} + L_2^2\left(1 - (1-p_2)^{L_2-1}\right) \tag{17}$$

and

$$\beta_5 = L_2 - 1 - (1-p_2)\left(1 - (1-p_2)^{L_2-1}\right)/p_2. \tag{18}$$

2) $L_k \cdot p_k \geq 1$: If $L_k \cdot p_k \geq 1$, (14)–(16) are inaccurate since $E(X_q) = \sum_i (X_q = i) \cdot P_{X_q}(i)$ is infinite. Then, two cases can be distinguished in the following.

1) $L_k \cdot p_k > 1$, which implies the preselected L cannot provide enough LEC PDUs to recover the lost information PDUs. Once the status update enters busy stage, the lost information PDUs will backlog at the receiver until the sender starts retransmission. In this case, only X_1 exists, and the probability of X_1 starts from the ith information PDU in the $(j+1)$th L-interval equals $P_{D,1} = p_k(1-p_k)^{j(L_k-1)+i-1}$, which represents the second term in (25) and the second and fourth terms in (26), both shown at the bottom of the page. Moreover, there are R_{lr} intervals in X_1, which can be expressed as $R_{lr} = n/(L_k-1) - j - 1$, and the total number of PDUs R_{tp} and the number of information PDUs R_{ip} in X_1 are $R_{tp} = R_{lr} \cdot L_k + L_k - i$ and $R_{ip} = R_{lr} \cdot (L_k - 1) + L_k - i - 1$, respectively. Thus, the number of extra LEC PDUs in the retransmission to recover the lost PDUs is $R_{nd} = (R_{ip} \cdot p_k - R_{lr} \cdot (1-p_k))/(1-p_k)$. Therefore, the total delay time for all information PDUs in R can be written as

$$E_1 = \left(R_{ip} + 1\right) \cdot \left((R_{nd} + 1) \cdot t_{s_1} + 2t_r + R_{tp} \cdot \left(t_{s_1} \cdot \eta_1 + t_{s_2} \cdot \eta_2\right)\right). \tag{19}$$

The delay time in D without and with considering D_f in R can be expressed as follows:

$$E_2 = \left(\frac{R_{ip} \cdot \left(R_{ip}+1\right)}{2} - \frac{R_{lr} \cdot (R_{lr}+1) \cdot L_2}{2}\right) \cdot t_{s_2} + R_{ip} \cdot (R_{nd}+1) \cdot t_{s_2} + 2t_r \tag{20}$$

and

$$E_3 = E_2 + P_{D,1} \cdot E\left(Q_m^1\right) \cdot t_{s_1} \cdot \left(R_{tp} - E\left(Q_m'\right) + 1\right). \tag{21}$$

2) $L_k \cdot p_k = 1$, which means that the number of lost PDUs is exactly equal to that of LEC PDUs in the long-term average. Since the PDU lost follows i.i.d., the transmission is actually the same as (i) unless there exactly only one PDU is lost, i.e., $X_q = 1$. Thus, if $X_q = 1$, the probability of X_q starts from the ith information PDU in the $(j+1)$th L-interval is $P_{D,2} = p_k(1-p_k)^{j(L_k-1)+L_k-1} \cdot (1-p_k)^{L_k-i}$. Otherwise, the probability is $P_{D,3} = p_k(1-p_k)^{j(L_k-1)+i-1} \cdot (1-(1-p_k)^{L_k-i})$, which is the first term in (25) and the first and third terms in (26), respectively. Furthermore, the delay time in R when $X_q = 1$ can be written as

$$E_4 = (L_1 - i + 1) \cdot (L_1 - i) \cdot \left(t_{s_1} \cdot \eta_1 + t_{s_2} \cdot \eta_2\right). \tag{22}$$

The delay time in D when $X_q = 1$ with and without considering D_f in R are given as follows:

$$E_5 = \frac{(L_2 - i + 1) \cdot (L_2 - i)}{2} \cdot t_{s_2} + P_{D,1} \cdot E\left(Q_m^1\right) \cdot t_{s_1} \cdot (L_2 - i + 1) \tag{23}$$

and

$$E_6 = E_4 - P_{D,1} \cdot E\left(Q_m^1\right) \cdot t_{s_1} \cdot (L_2 - i + 1). \tag{24}$$

Therefore, we can assume that there are at most two X_q for $L_k \cdot p_k \geq 1$, and if X_2 exists, $X_1 = 1$. Let $pos = (n - E(Q_m') \cdot [L_1 - 1/L_1)] \cdot (1 + [1/L_2 - 1)]/[L_2]$ denote the position of PDUs at D, i.e., the boundary of whether D_S is affected by D_f, and the approximate expectation of forwarding delay and service delay can be derived in (25) and (26).

$$\lim_{n\to\infty} \frac{1}{n}\left(\sum_{i=1}^{n} D_f(i)\right) \approx \frac{1}{n} \sum_{j=0}^{n/(L_1-1)-1} \sum_{i=1}^{L_1-1} \left(P_{D,3} \cdot E_1 + P_{D,2} \cdot E_4\right) + P_{D,2} \sum_{m=j+1}^{n/(L_1-1)-1} \sum_{n=1}^{L_1-1} P_{D,1} \cdot E_1 \tag{25}$$

$$\lim_{n\to\infty} \frac{1}{n} E\left(\sum_{i=1}^{n} D_s(i)\right) \approx \frac{1}{n} \sum_{j=0}^{\lceil pos\rceil} \sum_{i=1}^{L_2-1} \left(P_{D,3} \cdot E_2 + P_{D,2} \cdot E_3\right) + P_{D,2}\left(\sum_{m=j+1}^{\lceil pos\rceil} \sum_{z=1}^{L_2-1} P_{D,1} \cdot E_2 + \sum_{m=\lceil pos\rceil+1}^{n/(L_2-1)} \sum_{z=1}^{L_2-1} P_{D,1} \cdot E_3\right) + \frac{1}{n} \sum_{j=\lceil pos\rceil+1}^{n/(L_2-1)-1} \sum_{i=1}^{L_2-1} \left(P_{D,3} \cdot E_5 + P_{D,2} \cdot E_6\right) + P_{D,2}\left(\sum_{m=j+1}^{n/(L_2-1)-1} \sum_{z=1}^{L_2-1} P_{D,1} \cdot E_3\right) \tag{26}$$

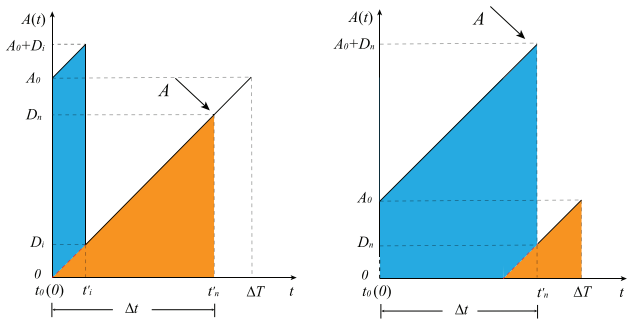

Fig. 4. AoI evolution model of a status update transmission. (a) AoI evolution with the first PDUs has been upload before the transmission is completed. (b) AoI evolution with all PDUs upload together at the end.

Finally, the expected end-to-end delay of D-LEC-f CFDP scheme can be calculated by substituting (14), (16), (25), and (26) into (6).

B. Peak AoI

Assume that S generates a status update in each $\triangle T$, let $A_0 = \triangle T$ denote the initial AoI of a status update at S, and $\triangle t$ denotes the time elapses from the generation of a status update to upload all the information PDUs at D, respectively. We define the generation time of each information PDU d_i is $t_i = t_0$, and t_i' is the time when d_i is successfully uploaded at D. Therefore, D_i can be written as $D_i = t_i' - t_0$, and $D_n = \triangle t$ is the delay time of the last information PDU.

Moreover, to achieve higher timeliness, we assume that S, R and D are ruled by last-come–first-served (LCFS) policy that discarding the current status update if it has not been uploaded to the application layer in D when the next status update has been collected by S [27], and the PAoI of the last status update is $2\triangle T$ and resetting AoI to A_0. Therefore, the AoI evolution of each status update transmission in the D-LEC-f CFDP scheme is shown in Fig. 4, which can be divided into two cases.

If the first information PDU d_1 can be uploaded before all PDUs at D as shown in Fig. 4(a), we set this AoI evolution case as State 1. Otherwise, if all information PDUs are uploaded at t_n' as shown in Fig. 4(b), we denote this AoI evolution case as State 2. Then, the expression of PAoI A for the D-LEC-f CFDP scheme can be written as

$$A = \begin{cases} D_n, & \text{State 1} \\ A_0 + D_n, & \text{State 2.} \end{cases} \tag{27}$$

Therefore, the expectation of A can be derived as

$$E(A) = D_n + \Pr\{\text{State 2}\} \cdot A_0. \tag{28}$$

Let $\hat{N}_k$ and T_{fe}^k denote the total number of transmitted PDUs and feedback delay in the kth hop transmission, respectively. Note that D_n depends on the total number of PDUs transmitted by S, the number of PDUs remain ought to be transmitted by R after the first hop and the feedback delay between R and D, which are denoted as $\hat{N}_1$, $\hat{N}_r$, and T_{fe}^2, respectively. Thus, D_n can be further expressed as $D_n = 2t_r + \hat{N}_1 + \hat{N}_r + T_{re}^2$, and the expectation of $\hat{N}_2$ and T_{fe}^2 are

$$E\left(\hat{N}_1\right) = n + \frac{n}{L_1 - 1} \sum_{i=0}^{\left\lfloor \frac{n(1-p_1)}{L_1-1} \right\rfloor} C_n^i \cdot p_1^i \cdot (1-p_1)^{n-i} + \sum_{i=\left\lfloor \frac{n(1-p_1)}{L_1-1}+1 \right\rfloor}^{n} i \cdot C_n^i \cdot p_1^i \cdot (1-p_1)^{n-i-1} \tag{29}$$

and

$$E\left(T_{fe}^2\right) = \sum_{i=\left\lfloor \frac{n(1-p_2)}{L_2-1}+1 \right\rfloor}^{n} \left(2t_r + t_{s_2}\right) \cdot C_n^i \cdot p_2^i \cdot (1-p_2)^{n-i-1}. \tag{30}$$

Moreover, it can be easily concluded that $\hat{N}_r$ equal to the sum of the queue length caused by X_m in R and the number of extra LEC PDUs transmitted in the second hop retransmission, i.e., $\hat{N}_r = Q_m' \cdot [L_2(L_1-1)/L_1(L_2-1) + (E(\hat{N}_2) - n - [n/L_2 - 1)]$. Since the second term of (28) depends on the value of X_1, we define a random variable X_a as the number of transmitted LEC PDUs in X_1 that failed to receive the first PDU at D. Therefore, the probability distribution of X_a is given as follows [33]:

$$P_{X_a}(x_a) = \begin{cases} 1 - p_2, & \text{for } x_a = 0 \\ p_2(1-p_2)^{L_2-1}, & \text{for } x_a = 1 \\ \frac{L_2-1}{x_a-1} p_2^x (1-p_2)^{L_2-1} \binom{x_a L_2 - 2}{x_a - 2}, & \text{for } x_a \geq 1. \end{cases} \tag{31}$$

Thus, the probability of State 2 can be expressed as

$$\Pr\{\text{State 2}\} = 1 - \sum_{i=0}^{n/(L_2-1)} \Pr(x_a = i). \tag{32}$$

Finally, by substituting (10), (29), (30), and (32) into (28), the closed-form expectation of PAoI can be further written as follows:

$$E(A) = 2t_r + \Pr\{\text{State 2}\} \cdot A_0 + E\left(T_{fe}^2\right) + t_{s_1} \cdot E\left(\hat{N}_1\right) + t_{s_2} \cdot E\left(\hat{N}_r\right). \tag{33}$$

IV. Optimization of A-LEC-f CFDP

In this section, we formulate a POMDP problem to achieve further lower PAoI and end-to-end delay, and solve it with a lower complexity PIB algorithm for the A-LEC-f CFDP scheme.

A. POMDP Formulation

The POMDP problem in our A-LEC-f CFDP scheme can be described by a tuple $<S, Z, A, T_r, R, O, b>$, and each parameter is introduced as follows.

S: S is the state space, where $s_t^1 = (m, \omega, d)$ denotes that $m(0 \leq m \leq n)$ information PDUs have been transmitted, $\omega(d < \omega \leq m)$ information PDUs are backlogged in the queue at R, which needs $d(0 \leq d < \omega)$ successfully received PDUs to be recovered at t in the first hop, while $s_t^2 = (m, \delta)$ denotes

that $m(0 \le m \le n)$ information PDUs have been transmitted, and $\delta(0 \le \delta < m)$ information PDUs in D need to be recovered at t in the second hop.

Z: Z is the set of observations, where $z_{t-2t_r} = \delta$ implies that the system can observe δ lost information PDUs in the receiver at $t - 2t_r$.

A: A is the set of possible actions to be taken by the system, where $A = \{L_k^1, \ldots, L_k^r, \ldots, L_k^{T+1}\}$, and $a_t = L_k^r$ indicates the sender selects $L_k^r = r$ in kth hop at t.

T_r: $S \times A \times S \to \mathbb{T}$ denotes the state transition function, where $T_r(s_t, a_t, s_{t+T})$ denotes the probability of transiting to the next state $s_{t+T} \in S$ under the current state $s_t \in S$ and action $a_t \in A$ at t.

R: $S \times A \to \mathbb{R}$ is the reward function, with $R(s_t, a_t)$ representing the immediate reward for taking action a_t in state s_t.

O: $S \times A \times Z \to \mathbb{O}$ represents the observation function, where $O(s_t, a_{t-T}, z_{t-2t_r})$ gives the probability for observing z_{t-2t_r} at S or R, when it reaches s_t under action a_{t-T}.

b: b is the belief state in each state, where $b_t(s_t)$ denotes the probability distribution of being in each state $s_t \in S$, and it satisfies $\sum_{s_t \in S} b_t(s_t) = 1$.

Note that we can replace s_t and s_{t+T} with s and s', respectively, by ignoring the subscripts t and $t+T$, which can also be used for a, z and b. Then, the next belief state b' can be calculated as follows:

$$b'(s) = \frac{O(s, a_{t-T}, z) \sum_{s' \in S} T_r(s', a_{t-T}, s) b(s')}{\sum_{s \in S} O(s, a_{t-T}, z) \sum_{s' \in S} T_r(s', a_{t-T}, s) b(s')}. \quad (34)$$

Denote $V^*(b)$ is the optimal value of belief state b, which can represent the maximum long-term reward based on the following optimal policy π^*, and can be expressed as [39]:

$$V^*(b) = \max_{a \in A} \sum_{s \in S} \left\{ b(s) R(s, a) + \sum_{z' \in Z} O(s', a, z') V^*(\tau(b, a, z')) \right\} \quad (35)$$

where $\tau(b, a, z')$ is the updated belief state function in (34). Moreover, the optimal policy π^* that can obtain the maximum expected cumulative return for the POMDP problem is also necessary. Thus, given the optimal value function V^*, the optimal policy π^* can be expressed as [40]

$$\pi^*(b) = \max_{a \in A} \sum_{s \in S} \left\{ b(s) R(s, a) + \sum_{s' \in S} T_r(s, a, s') V^*(\tau(b, a, z')) \right\}. \quad (36)$$

Furthermore, in order to calculate $V^*(b)$ with large belief space, (35) can be further expressed by the point-based value iteration (PBVI) as follows [29]:

$$V^*(b) = \max_{a \in A} \sum_{s \in S} \left\{ b(s) R(s, a) + \sum_{z' \in Z} \max_{\phi_t^i \in \Phi} (b_t \cdot \phi_t(s)) \right\} \quad (37)$$

where $\{\phi_t^i\} \in \Phi$ is a set of linear vectors that is the maximizing element of $V^*(b)$ for fixed action a_t, observation o and belief state b_t, which can be written as

$$\phi_t^{i+1}(s) = \sum_{s' \in S} O(s', a, z') \times \sum_{s \in S} T_r(s, a, s') b_t(s) \phi_t^i(s). \quad (38)$$

However, its complexity still increases dramatically with the state space, and hence is not suitable for the code design problem considered in this POMDP. Thus, we design a low-complexity algorithm called the PIB that measures the optimal value function with the upper bound directly based on PBVI for the considered POMDP in the following section.

B. PIB Algorithms

In this section, some details of PIB are described. First, we set the reward function according to (33). Note that when $T = 1$, the time between generation and forwarding of a PDU in the first hop equals the end-to-end delay of first hop, which means the reward function of this hop can be measured by it. Considering the function is smaller than real delay when $T > 1$, we can increase the weight of the impact of backlogged PDUs. Meanwhile, we only need to consider the number of PDUs that remain ought to be transmitted by R at time t in the second hop, if the initial AoI is ignored. Therefore, the immediate reward function of both two hops can be, respectively, expressed as

$$R(s_t, a_t) = \begin{cases} -(n - m + 0.5L\omega), & \text{first hop} \\ -(n - m + \delta), & \text{second hop.} \end{cases} \quad (39)$$

Considering the optimal belief value of POMDP is difficult to solve, and it is related to the optimal state values $V^*(s)$ as

$$V^*(b_t) \le V^U(b_t) = \sum_{s \in S} b_t(s) V^*(s). \quad (40)$$

If the POMDP turns to fully observable, i.e., Markov decision process (MDP), the optimal state value of the first hop $V_{\text{MDP}}^{\text{first}*}$ and second hop $V_{\text{MDP}}^{\text{sec}*}$ can be easily determined by immediate reward function and transition function as follows:

$$V_{\text{MDP}}^{\text{first}*}(m, \omega, d) = -\frac{(n - m + 0.5L \cdot \omega)(\omega - d)}{1 - p_1} - \frac{(n - m + \delta)(n - m)}{2(1 - p_1)} \quad (41)$$

and

$$V_{\text{MDP}}^{\text{sec}*}(m, \delta) = -\frac{(n - m + (1 + \delta))\delta}{1 - p_2} - \frac{(n - m + 1)(n - m)}{2(1 - p_2)}. \quad (42)$$

Thus, the upper bound of belief value can be found by taking (41) and (42) into (40), which can be used to approximate the optimal belief value.

Furthermore, since the probability of State 2 needs to be minimized, the policy at the initialization stage must be conservative, i.e., the lower bound of the optimal value function can be used for initialization procedure. Therefore, given the belief state b_t^1, all the subsequent b_t^i can be determined by L, until transmitting all information PDUs, i.e., reaching b_t^n, and its optimal value $V^L(b_t^n)$ can be expressed as

$$V^L(b_t^n) \doteq V^L(n, \delta) = -\frac{(1 + \delta) \cdot \delta}{2(1 - p_k)}. \quad (43)$$

Mathematically, the lower bound of the belief value is

$$V^L(b_t) = \max_{a_t \in A} \sum_{s \in S} b_t(s) R(s_t, a_t) + V^L(b_{t+T}). \quad (44)$$

Algorithm 1: A-LEC-f CFDP Scheme

Input: b, S, Z, $\overline{V}$, $\underline{V}$, T, p, n, π,
Output: The optimal policy of the first or second hop transmission
initialization: $A = [L_k^1, L_k^2, ..., L_k^{T+1}]$, $\underline{V} = [V_1^L, V_2^L, ..., V_{T+1}^L]$;
for $i = 1$ *to* $T+1$ **do**
  update b_i^m with the selected action a_i,
  compute the reward R_i^m under b_i^m;
  while $m' \le n$ **do**
    compute the value $V_i^L(m)$ with (b_i^m, R_i^m),
    update m to m', b_i^m to $b_i^{m'}$;
  end
  compute the lower bound V_i^L under a_i with $V_i^L = \sum_m V_i^L(m) + V_i^L(n)$.
end
$a_1 = \max_{a \in A} \underline{V}$, $\pi = [\pi \ a_1]$.
while $m \le n$ **do**
  $a_i = \text{PIB}(m, p, T, \pi, \delta, \omega, d)$, update m, π, δ *or* ω, d.
end
return π

Algorithm 2: Function: $a_i = \text{PIB}(m, p, T, \pi, \delta, \omega, d)$

Input: $m, p, T, \pi, \delta, \omega, d$
Output: The optimal policy of next feedback interval
initialization:calculate s with δ *or* ω, d, and update b with (s, a, z);
initialization:$\overline{V} = [V_1^U, V_2^U, ..., V_T^U, V_{T+1}^U]$, $T \le n$;
for *every* $a_i \in A$ **do**
  for *every* $z_j \in Z$ **do**
    update b' with the selected group (b, a_i, z_j),
    compute V_{ij}^U under the belief state b';
  end
  compute the upper bound V_i^U under a_i with $V_i^U = \sum_{z_j \in Z} O(s, a_i, z_j) \cdot V_{ij}^U$.
end
$a_i = \max_{a \in A} \overline{V}$.
return a_i

Therefore, we utilize the above policy to design an PIB algorithm and solve the POMDP problem in our A-LEC-f CFDP scheme, which is summarized in Algorithms 1 and 2 in detail. The complexity analysis of our PIB algorithm is given in Section V.

V. Simulation Results and Discussions

In this section, we present the simulation results to evaluate the performance of our proposed D-LEC-h, D-LEC-f, and A-LEC-f CFDP schemes, and the main parameters are shown in Table II. Moreover, the BER performance is significantly different under the infrequent light shadowing (ILS), average shadowing (AS), and frequent heavy shadowing (FHS) SR fading parameters, depending on different elevation angle, altitude, etc., which is summarized in Table III.

The BER of our LEC-CFDP scheme with different diversity gains N under FHS, ILS and AS SR fading parameters are shown in Fig. 5(a), and validate the accuracy of our SR fading channel model. Moreover, the result also shows that the SR channel with FHS needs multiple antennas to guarantee reliable transmission compared to the ILS and AS fadings. Then, as shown in Fig. 5(b), we simulate the BLER performance with $N = 8$, $B = 200, 500, 1000$ bytes under FHS and $N = 1$, $B = 200$ bytes under ILS and AS. We can observe that although the BLER of FHS increases with the PDU size, it is smaller than the ILS with 200 bytes when PDU size reaches 1 kB and SNR $\ge$ 8.5 dB, while the BER of FHS can only achieve it when SNR $\ge$ 10 dB, which demonstrates that the reliable transmission of 1-kB PDU under $N = 8$ with LEC can be ensured. Thus, we utilize FHS and $N = 8$, $B = 1000$ bytes

TABLE II
Simulation Parameters

Type	Parameters	Value
SR fading channel	Average power of scatter component b_0	0.063
	Average power of LoS component Ω	0.000897
	Nakagami-m parameter m	1
transmission system	PDU size B (bytes)	[200, 500, 1000]
	Status update size n	[60, 100]
	LEC intervals L_k	[2, 3, 5, 11]
	Feedback delay T	[3, 6, 12, n]
	Distance d	300 km
	Status update interval $\triangle T$	900 ms
	Initial AoI A_0	900 ms
	Time slot t	1 ms
	Propagation delay t_r	1 ms
	Uplink transmission delay t_{s_1}	1.5 ms
	Downlink transmission delay t_{s_2}	1 ms

TABLE III
Shadowed-Rician Fading Parameters

shadowing	b_i	Ω_i	m_i
Infrequent light shadowing (ILS)	0.158	1.29	20
Average shadowing (AS)	0.126	0.835	11
Frequent heavy shadowing (FHS)	0.063	0.000897	1

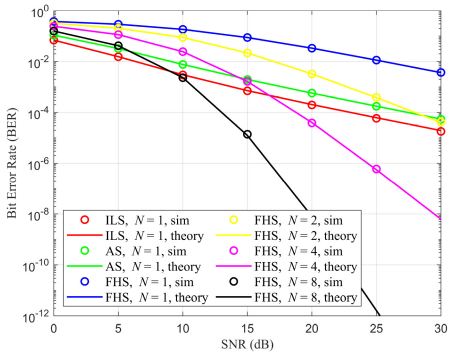

(a)

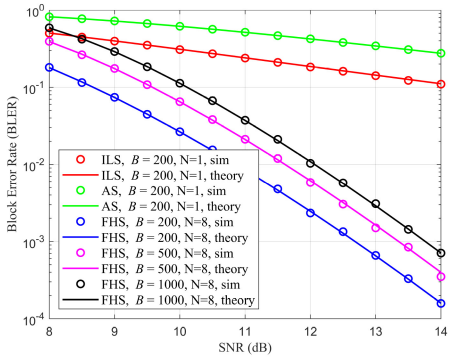

(b)

Fig. 5. BER with QPSK and different diversity gains N under ILS, AS, and FHS, and the BLER performance for N and SR fading parameters under different PDU size. (a) BER versus transmission SNR. (b) BLER versus transmission SNR.

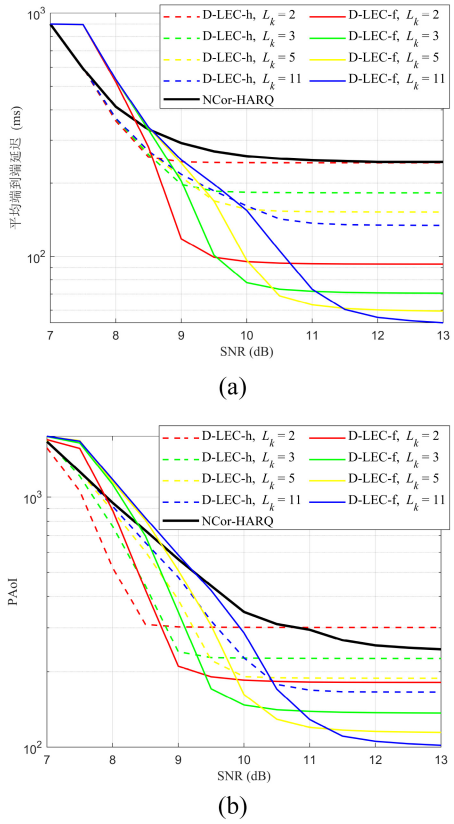

Fig. 6. Comparison of D-LEC-h CFDP, D-LEC-f CFDP, and NCor-HARQ scheme, the number of information PDUs is $n = 60$. (a) End-to-end delay versus transmission SNR. (b) PAoI versus transmission SNR.

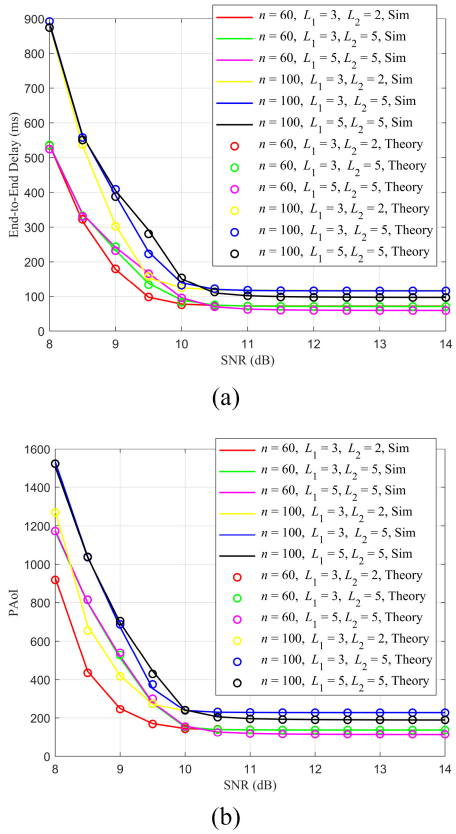

Fig. 7. Performance of D-LEC-f CFDP scheme with different n and (L_1, L_2). (a) End-to-end delay versus transmission SNR. (b) PAoI versus transmission SNR.

in the following simulations to reflect the effectiveness of our proposed schemes.

We simulate the D-LEC-h CFDP and D-LEC-f CFDP with $L_k = 2, 3, 5, 11$ to evaluate the performance of two schemes, and compare with an age-optimal transmission scheme for dual-hop called NC HARQ with one-time retransmission (NCor-HARQ) [23] in Fig. 6. Specifically, the D-LEC-h CFDP scheme has lower expected end-to-end delay and PAoI than the D-LEC-f CFDP scheme when SNR $\leq$ 8.5 dB as shown in Fig. 6(a) and (b). However, their performance will reverse if SNR $\geq$ 8.5 dB. The reason is that when SNR is higher, R can receive more PDUs successfully, which enable itself to forward faster, and the reception and transmission of the D-LEC-f CFDP are carried out at the same time, while that of the other are separate. In the low SNR region, the BLER of the D-LEC-f CFDP is little higher than the D-LEC-h CFDP due to the high SI, which can be represented as αP, where P is the normalized transmit power of the satellite and $\alpha = 0.1$ is the SI cancelation quality parameter [35]. Moreover, it can observe that our D-LEC CFDP scheme always outperform the NCor-HARQ scheme in different SNR regions. The main reason is that the LEC construction in the D-LEC CFDP can accelerate the recovery of lost PDUs, particularly when L_k is small, while the LEC PDUs in the NCor-HARQ are transmitted after all information PDUs have been sent. Furthermore, when SNR $\geq$ 11 dB, the PAoI of NCor-HARQ gradually lower than the D-LEC-h CFDP with $L_k < 3$, i.e., $L_1 = L_2 < 3$ as shown in Fig. 6, since the receivers need less LEC PDUs to recover the lost PDUs in a high SNR region. However, benefiting by the full-duplex relay mode, the D-LEC-f CFDP scheme can still outperform the NCor-HARQ scheme in this case.

Then, we simulate the D-LEC-f CFDP scheme with three different parameters of L_1 and L_2 to validate the accuracy of our derivations as shown in Fig. 7. We can observe that the theoretical derivations of expected end-to-end delay in (6) and PAoI in (33) are agreed well with the simulation results in Fig. 7(a) and (b), respectively. Moreover, we can observe that there is an optimal group (L_1, L_2) that enables the D-LEC CFDP scheme to achieve the best performance in different SNR regions. For example, When $(L_1 = 3, L_2 = 2)$ and SNR = 9 dB, both two parameters fall to the floor region. Thus, if L_k, especially L_2, is too large or too small in a specific SNR region, the PAoI and end-to-end delay will both increase due to the retransmission or redundant LEC PDUs. This also requires us to design the A-LEC-f CFDP to update the optimized L_k to improve the timeliness.

In Fig. 8(a) and (b), we can observe that the A-LEC-f CFDP scheme greatly outperforms the D-LEC-f CFDP scheme in both PAoI and end-to-end delay. The main reason is the A-LEC-f CFDP can reselect an appropriate L_k to adapt to the varying CSI according to the delayed feedback NAK, especially in a low SNR region. Thus, R can effectively predict

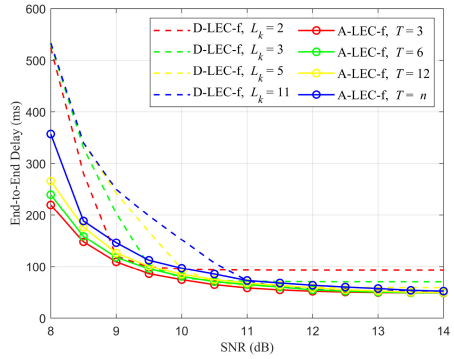

(a)

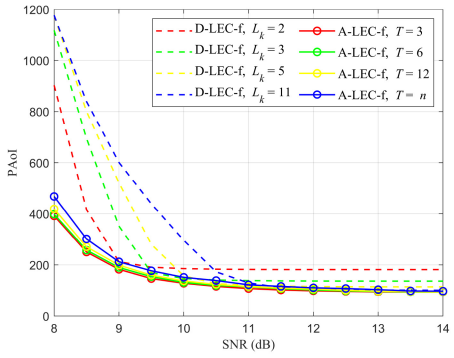

(b)

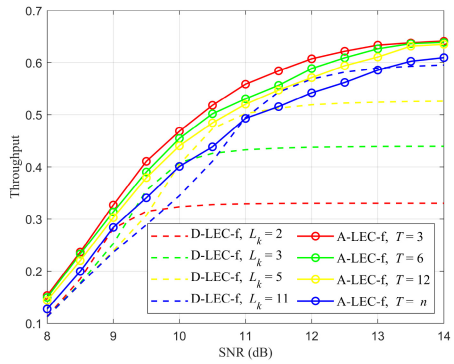

(c)

Fig. 8. Comparison of D-LEC-f CFDP and A-LEC-f CFDP schemes, the number of information PDUs is $n = 60$. (a) End-to-end delay versus transmission SNR. (b) PAoI versus transmission SNR. (c) Throughput versus transmission SNR.

CSI to avoid retransmission, which greatly improves the performance of the D-LEC-f CFDP in bad channel condition. Furthermore, the performance of these two schemes is similar when SNR $\geq$ 11 dB, because the minimum value of these two parameters mainly depends on the number of information PDUs when channel is always in good state. Moreover, we also compare the difference of throughput between two schemes and the performance versus SNR as shown in Fig. 8(c), and the expectation of throughput can be calculated as follows:

$$\tau = \frac{\text{Number of information PDUs}}{\text{Expected of transmission time}} = \frac{n}{E(A')} \tag{45}$$

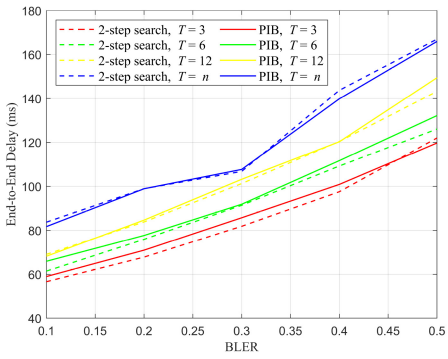

(a)

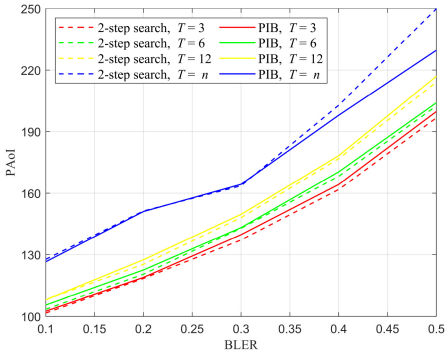

(b)

Fig. 9. Performance of A-LEC-f CFDP scheme by optimizing via PIB and 2-step search algorithm. (a) Average end-to-end delay versus BLER. (b) PAoI versus BLER.

where

$$E(A') = E(A) - \Pr\{\text{State } 2\} \cdot A_0. \tag{46}$$

It can be observed that the throughput of two schemes is similar when SNR$\leq$ 10 dB. Moreover, the A-LEC-f CFDP can obviously achieve higher throughput when SNR $\geq$ 10 dB. However, if T is too large, L_k is adjusted by the sender may deviate from the optimal policy to a certain extent, which may lead to obviously decreasing of throughput. As shown in Fig. 8(c), when the D-LEC-f CFDP scheme approaches the maximum throughput, it is better than that of the A-LEC-f CFDP scheme when $T = n$.

Finally, we simulate the expected end-to-end delay and PAoI of the A-LEC-f CFDP scheme by optimizing via PIB, and compare with the D-step search algorithm that can achieve near-optimal solutions for the POMDP problem [41] as shown in Fig. 9(a) and (b), and take the illustrative case of 2-step search. We can observe that both two performance parameters of POMDP solved by two algorithms is similar, and the smaller the feedback interval T leads to better performance of our schemes. Moreover, the tight upper bound of $V^*(b)$ is given in (41) and (42) and show that the complexity of our PIB is low. Specifically, the number of states is $O(|S^1|) = O(n^3)$ in the first-hop transmission, and $O(|S^2|) = O(n^2)$ in the second-hop transmission. Since the belief state b is restricted by S, the maximum number of greedy search is the same as S^k in kth hop transmission, while the number of actions is $O(|A|) = O(T)$

and the number of observations is $O(|Z|) = O(T)$ in each hop for POMDP. Therefore, the complexity of PIB algorithm is $O(T^2 \cdot n^6)$. On the other hand, the complexity of D-step search algorithm is $O(T^{2D} \cdot n^{12})$ [42].

VI. Conclusion

In this article, we modeled an age-critical dual-hop LEC-CFDP transmission scheme in S-IoT, in which a UE S transmitted the collected status updates with multiple PDUs to the relay satellite R, then R selected an appropriate relay mode to forward the re-encoded PDUs to the ground station D. Then, we proposed two D-LEC CFDP schemes to improve the PAoI and expected end-to-end delay with half-duplex and full-duplex relay modes, respectively, and introduced them in detail. Furthermore, we further analyzed the D-LEC-f CFDP scheme, and derived an approximated expression for expected end-to-end delay and a closed-form expression for PAoI in the D-LEC-f CFDP scheme. Moreover, we utilized the results to preselect an appropriate L to improve the timeliness. Furthermore, we proposed the A-LEC-f CFDP scheme and formulated a POMDP problem to achieve the lowest PAoI, and solved it through our low-complexity PIB algorithm. Simulation results validated the accuracy of our theoretical derivations of expected end-to-end delay and PAoI, and showed that the A-LEC-f CFDP scheme can greatly lower the PAoI and end-to-end delay than the D-LEC-f CFDP scheme and state-of-the-art scheme, as well as higher throughput. Finally, it is worthy of noting that our work will shed important light on the timely multihop transmission design for the mega-constellation LEO satellite networks, such as Starlink and OneWeb.

Appendix A
Derivation of the Average Backlogged Queue

Consider N_t^k PDUs are transmitted in the k-hop transmission at time t, which can be divided into $\lceil N_t^k/L \rceil$ L-intervals. According to the definition of X_q, we assume that the qth backlogged queue is consisted of X_q L-intervals. Since $\{X_1, X_2, \ldots, X_q\}$ is a sequence of random positive integers in (7), the recovering process of a status update can be modeled as a renewal process, where X_q is the qth renewal interval. Define T_q as $T_q = \sum_{i=1}^{q} X_i, q > 0$ and the renewal interval $[T_q, T_{q+1}]$ is the number of L-interval in a recovering process. Then the random variable $(N_t^k)_{t\geq 0}$ given by $Y_t = \sup\{q : T_q \leq t\}$ represents the number of L-intervals in a status update transmission until time t.

In each recovering process of the k-hop transmission in a status update, define $Q_1^k, Q_2^k, \ldots, Q_q^k$ as a sequence of i.i.d. random variables denoting the sum-length of the backlogged queue $(X_q - 1)L_k + B_q$ for all PDUs, i.e., Q_q^k is the sum of the number of PDUs in the qth backlogged queue. Thus, the transmission can be divided into two cases for analysis in the following.

1) $X_q = B$, which means the backlogged queue only depends on B_q.
2) $X_q \geq 1$, and the queue length of each information PDU is the same as $(X_q - 1)L_k + B_q$.

Therefore, the sum-length of $(X_q - 1)L_k + B_q$ for all information PDUs in a backlogged queue can be expressed as

$$\begin{aligned}&\sum_{i=1}^{(X_q-1)L_k} (X_q-1)L_k - \sum_{i=1}^{X_q-1} (X_q-1)L_k \\ &\quad + \sum_{i=1}^{L_k-1} p_k(1-p_k)^{i-1}(L_k-i)\big(X_qL_k - i + 1\big) \\ &= \Big(X_q^2 - 2X_q + 1\Big)(L_k-1)L_k + X_q\beta_1^k + \beta_2^k. \end{aligned} \tag{47}$$

Let $Z_t^k = \sum_{j=1}^{Y_t} Q_q^k$ denote a renewal–reward process, and its expectation is the total length of the backlogged queues for all information PDUs until time t. According to the elementary renewal theorem for renewal–reward processes [33], we have $\lim_{t\to\infty}(1/t)E(Z_t^k) = [E(Q_q^k)/E(X_q)]$. Moreover, base on the above analysis of Q_q^k, we have $E(Q_q^k) = \sum_{i=1}^{\infty} E(Q_q^k|X_q = i)\Pr(X_q = i) = (E(X_q^2) - 2E(X_q) + 1)(L_k - 1)L_k + E(X_q)\beta_1 + \beta_2$. Since we assumed that $N_t^k = tL_k$, we have

$$\begin{aligned}\lim_{N_t^k\to\infty} \frac{1}{N_t^k} E\Big(Z_t^k\Big) &= \frac{\Big(E\Big(X_q^2\Big) - 2E\big(X_q\big) + 1\Big)}{E\big(X_q\big)} \\ &\quad \cdot (L_k - 1) + \frac{E\big(X_q\big)\beta_1^k + \beta_2^k}{E\big(X_q\big)L_k}. \end{aligned} \tag{48}$$

Appendix B
Derivation of the Longest Backlogged Queue

If the number of transmitted PDUs is limited, the close-form expectation of the longest backlogged queue length can be derived. In this case, the maximum value of X_q is $n/(L_k - 1)$, and let $\bar{X}$ denote X_q with a upper bound $n/(L_k - 1)$, which also represents the qth renewal interval of a truncation renewal process. Therefore, the probability distribution of $\bar{X}$ can be expressed as

$$P_{\bar{X}}(\bar{x}) = \begin{cases} X_q, & \text{for } 0 < \bar{x} < n/(L_k - 1) \\ n/(L_k - 1), & \text{for } \bar{x} \geq n/(L_k - 1). \end{cases} \tag{49}$$

Then, we have

$$E\big(\bar{X}\big) = \sum_{i=1}^{n/(L_k-1)} i \cdot \Pr\big(X_q = i\big) + \frac{n}{L_k - 1} \cdot \Pr\Big(X_q > \frac{n}{L_k - 1}\Big). \tag{50}$$

In this case, the rounds of the renewal process is also finite, and its expectation is $E(Y_t) = m(t) = \sum_{s=1}^{\infty} P_s$, where P_s equals the convolution of s distribution function of $\bar{X}$. Moreover, $m(t)$ can be expressed by a simple form $M = [n/(L_k - 1)/E(\bar{X})]$ based on the renewal theorem.

According to the definition of X_m, we can find that all $\bar{x}$ that satisfy $M \cdot \Pr(\bar{x}) \geq 1$ must exist during a status update on average, and the maximum value $\bar{x}_{\max}$ of them equals the lower bound $\underline{X}$ of X_m. On the other hand, if $\bar{x}$ meets $M \cdot \Pr(\bar{x}) < 1$ and all $x_m \leq \bar{x}$ in this status update, $M \cdot \Pr(\bar{x})$ is the probability of $x_m = \bar{x}$. As a result, the probability distribution of X_m can

be expressed as

$$P(x_m) = \begin{cases} \prod_{i=\underline{X}+1}^{n/(L_k-1)} M \cdot \left(1 - \Pr(\bar{X} = i)\right), & \text{for } x = \underline{X} \\ M \cdot \Pr(\bar{X} = x_m), & \text{for } x_m > \underline{X} \cap \\ \prod_{i=x_m+1}^{n/(L_k-1)} M \cdot \left(1 - \Pr(\bar{X} = i)\right), & x_m \le n/(L_k - 1) \\ 0, & \text{otherwise.} \end{cases} \tag{51}$$

Since X_m is limited, its expectation $E(X_m) = \sum_i^{n/(L_k-1)} (X_m = i) \cdot P_{X_m}(i)$ can be directly calculated. Therefore, through the similar derivations to Appendix A, we can get the expectation of the longest backlogged queue length without retransmission as follows:

$$E\left(Q'_m\right) = (E(X_m) - 1)L_k + \beta_3^k. \tag{52}$$

Meanwhile, the retransmission time T_{re}^k in the k-hop transmission depends on the number of extra LEC PDUs and feedback delay, which implies its expectation can be obtained by combining (29) and (30) as follows:

$$E\left(T_{re}^k\right) = \left(E\left(\hat{N}_k\right) - n - \frac{n}{L_k - 1}\right) \cdot t_{s_k} + E\left(T_{fe}^k\right). \tag{53}$$

Finally, the longest backlogged queue for each hop transmission can be calculated by substituting (13), (52), and (53) into (10).

REFERENCES

[1] W. Saad et al., "A vision of 6G wireless systems: Applications, trends, technologies, and open research problems," *IEEE Netw.*, vol. 34, no. 3, pp. 134–142, May/Jun. 2020.

[2] J. Jiao, S. Wu, R. Lu, and Q. Zhang, "Massive access in the space-based Internet of Things: Challenges, opportunities, and future directions," *IEEE Wireless Commun.*, vol. 28, no. 5, pp. 118–125, Oct. 2021.

[3] J. Liu, Y. Shi, Z. M. Fadlullah, and N. Kato, "Space-air-ground integrated network: A survey," *IEEE Commun. Surveys Tuts.*, vol. 20, no. 4, pp. 2714–2741, 4th Quart., 2018.

[4] A. Kosta, N. Pappas, and V. Angelakis, "Age of information: A new concept, metric, and tool," *Found. Trends Netw.*, vol. 12, no. 3, pp. 162–259, 2017.

[5] S. Kaul, M. Gruteser, V. Rai, and J. Kenney, "Minimizing age of information in vehicular networks," in *Proc. Mesh Ad Hoc Commun. Netw.*, 2011, pp. 350–358.

[6] G. Wang, S. C. Burleigh, R. Wang, L. Shi, and Y. Qian, "Scoping contact graph routing scalability: Investigating the system's usability in space-vehicle communication networks," *IEEE Veh. Technol. Mag.*, vol. 11, no. 4, pp. 46–52, Dec. 2016.

[7] B. Soret, S. Ravikanti, and P. Popovski, "Latency and timeliness in multi-hop satellite networks," in *Proc. IEEE Int. Conf. Commun. (ICC)*, 2020, pp. 1–6.

[8] G. Yang, R. Wang, A. Sabbagh, K. Zhao, and X. Zhang, "Modeling optimal retransmission timeout interval for bundle protocol," *IEEE Trans. Aerosp. Electron. Syst.*, vol. 54, no. 5, pp. 2493–2508, Oct. 2018.

[9] R. Wang, A. Sabbagh, S. C. Burleigh, K. Zhao, and Y. Qian, "Proactive retransmission in delay-/disruption-tolerant networking for reliable deep-space vehicle communications," *IEEE Trans. Veh. Technol.*, vol. 67, no. 10, pp. 9983–9994, Oct. 2018.

[10] J. Ding, J. Jiao, S. Liu, S. Wu, and Q. Zhang, "Freshness-critical transmission scheme with IR-HARQ over multi-hop satellite-IoT," in *Proc. IEEE VTC-Fall*, Sep. 2021, pp. 1–5.

[11] "CCSDS file delivery protocol (CFDP)—Part 1: Introduction and overview," Nat. Aeronaut. Space Admin., Washington, DC, USA, Rep. CCSDS 720.1-G-4, 2021. [Online]. Available: https://public.ccsds.org/Pubs/720x1g4.pdf

[12] Z. Yang, H. Li, J. Jiao, Q. Zhang, and R. Wang, "CFDP-based two-hop relaying protocol over weather-dependent Ka-band space channel," *IEEE Trans. Aerosp. Electron. Syst.*, vol. 51, no. 2, pp. 1357–1374, Apr. 2015.

[13] "Erasure correcting codes for use in near-earth and deep-space communications," Nat. Aeronaut. Space Admin., Washington, DC, USA, Rep. CCSDS 131.5-O-1, 2014. [Online]. Available: https:// public.ccsds.org/Pubs/131x5o1.pdf

[14] M. A. Abd-Elmagid, N. Pappas, and H. S. Dhillon, "On the role of age of information in the Internet of Things," *IEEE Commun. Mag.*, vol. 57, no. 12, pp. 72–77, Dec. 2019.

[15] J. Jiao et al., "Age-optimal network coding HARQ transmission scheme for dual-hop satellite-integrated Internet," *IEEE Trans. Veh. Technol.*, vol. 70, no. 10, pp. 10666–10682, Oct. 2022.

[16] C. Xu, H. H. Yang, X. Wang, and T. Q. S. Quek, "Optimizing information freshness in computing-enabled IoT networks," *IEEE Internet Things J.*, vol. 7, no. 2, pp. 971–985, Feb. 2020.

[17] M. Moradian and A. Dadlani, "Age of information in scheduled wireless relay networks," in *Proc. IEEE Wireless Commun. Netw. Conf. (WCNC)*, 2020, pp. 1–6.

[18] N. Akar and O. Dogan, "Discrete-time queueing model of age of information with multiple information sources," *IEEE Internet Things J.*, vol. 8, no. 19, pp. 14531–14542, Oct. 2021.

[19] R. Wang, S. C. Burleigh, P. Parikh, C.-J. Lin, and B. Sun, "Licklider transmission protocol (LTP)-based DTN for cislunar communications," *IEEE/ACM Trans. Netw.*, vol. 19, no. 2, pp. 359–368, Apr. 2011.

[20] L. Shi et al., "Integration of reed-solomon codes to licklider transmission protocol (LTP) for space DTN," *IEEE Aerosp. Electron. Syst. Mag.*, vol. 32, no. 4, pp. 48–55, Apr. 2017.

[21] A. Cohen, G. Thiran, V. B. Bracha, and M. Médard, "Adaptive causal network coding with feedback for multipath multi-hop communications," *IEEE Trans. Commun.*, vol. 69, no. 2, pp. 766–785, Feb. 2021.

[22] J. Jiao, Z. Ni, S. Wu, Y. Wang, and Q. Zhang, "Energy efficient network coding HARQ transmission scheme for S-IoT," *IEEE Trans. Green Commun. Netw.*, vol. 5, no. 1, pp. 308–321, Mar. 2021.

[23] S. Liu, J. Jiao, Z. Ni, S. Wu, and Q. Zhang, "Age-optimal NC-HARQ protocol for multi-hop satellite-based Internet of Things," in *Proc. IEEE WCNC*, Nanjing, China, Mar. 2021, pp. 1–6.

[24] A. Sabbagh, R. Wang, S. C. Burleigh, and K. Zhao, "Analytical framework for effect of link disruption on bundle protocol in deep-space communications," *IEEE J. Sel. Areas Commun.*, vol. 36, no. 5, pp. 1086–1096, May 2018.

[25] J. Jiao, J. Zhou, S. Wu, and Q. Zhang, "Superimposed pilot code-domain NOMA scheme for satellite-based Internet of Things," *IEEE Syst. J.*, vol. 15, no. 2, pp. 2732–2743, Jun. 2021.

[26] G. Yao, A. Bedewy, and N. B. Shroff, "Age-optimal low-power status update over time-correlated fading channel," *IEEE Trans. Mobile Comput.*, early access, Mar. 16, 2022, doi: 10.1109/TMC.2022.3160050.

[27] J. Ding, J. Jiao, J. Huang, S. Wu, R. Lu, and Q. Zhang, "Age-optimal network coding HARQ scheme for satellite-based Internet of Things," *IEEE Internet Things J.*, vol. 9, no. 32, pp. 21984–21998, Nov. 2022.

[28] Y. Shao, Q. Cao, S. C. Liew, and H. Chen, "Partially observable minimum-age scheduling: The greedy policy," *IEEE Trans. Commun.*, vol. 70, no. 1, pp. 404–418, Jan. 2022.

[29] J. Pineau, G. J. Gordon, and S. Thrun, "Point-based value iteration: An anytime algorithm for POMDPs," in *Proc. Int. Joint. Conf. Artif. Intell.*, Aug. 2003, pp. 1–6.

[30] "Study on Narrow-Band Internet of Things (NB-IoT)/enhanced machine type communication (eMTC) support for non-terrestrial networks (NTN)," 3GPP, Sophia Antipolis, France, Rep. TR 36.763, V17.0.0, Jun. 2021.

[31] K. Storek, R. Schwarz, and A. Knopp, "Multi-satellite multi-user MIMO precoding: Testbed and field trial," in *Proc. IEEE Int. Conf. Commun. (ICC)*, 2020, pp. 1–7.

[32] "Solutions for NR to support non-terrestrial networks (NTN)," 3GPP, Sophia Antipolis, France, Rep. TR 38.821, V16.1.0., Jun. 2021.

[33] M. Karzand, D. J. Leith, J. Cloud, and M. Médard, "Design of FEC for low delay in 5G," *IEEE J. Sel. Areas Commun.*, vol. 35, no. 8, pp. 1783–1793, Aug. 2017.

[34] *Licklider Transmission Protocol (LTP) for CCSDS*, Space Data System Standard CCSDS 734.1-B-1, 2015. [Online]. Available: https://public.ccsds.org/Pubs/734x1b1.pdf

[35] Q. T. Ngo, K. T. Phan, W. Xiang, A. Mahmood, and J. Slay, "Two-tier cache-aided full-duplex hybrid satellite–terrestrial communication networks," *IEEE Trans. Aerosp. Electron. Syst.*, vol. 58, no. 3, pp. 1753–1765, Jun. 2022.

[36] A. Abdi, W. C. Lau, M.-S. Alouini, and M. Kaveh, "A new simple model for land mobile satellite channels: First- and second-order statistics," *IEEE Trans. Wireless Commun.*, vol. 2, no. 3, pp. 519–528, May 2003.

[37] M. K. Arti and S. K. Jindal, "OSTBC transmission in shadowed-Rician land mobile satellite links," *IEEE Trans. Veh. Technol.*, vol. 65, no. 7, pp. 5771–5777, Jul. 2016.
[38] F. P. Fontan, M. Vazquez-Castro, C. E. Cabado, J. P. Garcia, and E. Kubista, "Statistical modeling of the LMS channel," *IEEE Trans. Veh. Technol.*, vol. 50, no. 6, pp. 1549–1567, Nov. 2001.
[39] R. D. Smallwood and E. J. Sondik, "The optimal control of partially observable Markov processes over a finite horizon," *Oper. Res.*, vol. 21, no. 5, pp. 1071–1088, 1973.
[40] M. L. Littman, A. R. Cassandra, and L. P. Kaelbling, "Learning policies for partially observable environments: Scaling up," in *Proc. 12th Int. Conf. Mach. Learn. (ICML)*, Jul. 1995, pp. 362–370.
[41] X. Xu, Y. Zeng, Y. Li, and B. Vucetic, "Minimum-latency FEC design with delayed feedback: Mathematical modeling and efficient algorithms," *IEEE Trans. Wireless Commun.*, vol. 19, no. 11, pp. 7210–7223, Nov. 2020.
[42] S. Ross, J. Pineau, S. Paquet, and B. Chaib-Draa, "Online planning algorithms for POMDPs," *J. Artif. Intell. Res.*, vol. 32, pp. 663–704, Aug. 2008.

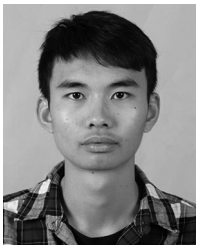

Jianhao Huang received the B.S. degree in communication engineering from Harbin Institute of Technology (Shenzhen), Shenzhen, China, in 2022, where he is currently pursuing the M.S. degree.

His current research interests include satellite communications and age of information.

Jian Jiao (Senior Member, IEEE) received the M.S. and Ph.D. degrees in communication engineering from Harbin Institute of Technology (HIT), Harbin, China, in 2007 and 2011, respectively.

From 2011 to 2015, he was a Postdoctoral Research Fellow with the Communication Engineering Research Centre, HIT Shenzhen (HITsz) Graduate School, Shenzhen, China. From 2016 to 2017, he was a China Scholarship Council Visiting Scholar with the School of Electrical and Information Engineering, The University of Sydney, Sydney, NSW, Australia. In 2017, he was with HITsz, where he has been a Professor with the Guangdong Provincial Key Laboratory of Aerospace Communication and Networking Technology, since 2022. He is also an Associate Professor with Peng Cheng Laboratory, Shenzhen. His current interests include semantic communications, satellite communications and networking, and coding techniques.

Prof. Jiao is currently serving as an Editor for *Science China Information Sciences*.

Ye Wang (Member, IEEE) received the M.S. and Ph.D. degrees in information and communication engineering from Harbin Institute of Technology (HIT), Harbin, China, in 2009 and 2013, respectively.

From 2013 to 2014, he was a Postdoctoral Research Fellow with the University of Ontario Institute of Technology, Oshawa, ON, Canada. From 2015 to 2021, he was an Assistant Professor with HIT Shenzhen, Shenzhen, China. Since 2022, he has been an Associate Professor with Peng Cheng Laboratory, Shenzhen. His research interests include satellite communications, resource allocation, and mobile Internet.

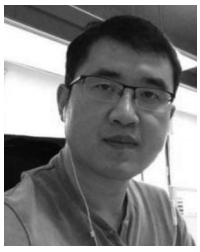

Shaohua Wu (Member, IEEE) received the Ph.D. degree in communication engineering from Harbin Institute of Technology, Harbin, China, in 2009.

From 2009 to 2011, he held a postdoctoral position with the Department of Electronics and Information Engineering, Shenzhen Graduate School, Harbin Institute of Technology (Shenzhen), Shenzhen, China, where he was an Associate Professor from 2012 to 2020. Since 2021, he has been a Professor with the School of Electrical and Information Engineering, Harbin Institute of Technology Shenzhen, and also a Professor with Peng Cheng Laboratory, Shenzhen. His current research interests include wireless image/video transmission, space communications, advanced channel coding techniques, and B5G wireless transmission technologies.

Rongxing Lu (Fellow, IEEE) received the Ph.D. degree from the Department of Electrical and Computer Engineering, University of Waterloo, Waterloo, ON, Canada, in 2012.

He is a Mastercard IoT Research Chair, a University Research Scholar, and an Associate Professor with the Faculty of Computer Science (FCS), University of New Brunswick (UNB), Fredericton, NB, Canada. Before that, he worked as an Assistant Professor with the School of Electrical and Electronic Engineering, Nanyang Technological University, Singapore, from April 2013 to August 2016. He worked as a Postdoctoral Fellow with the University of Waterloo from May 2012 to April 2013. His research interests include applied cryptography, privacy enhancing technologies, and IoT-big data security and privacy. He has published extensively in his areas of expertise.

Dr. Lu was awarded the most prestigious "Governor General's Gold Medal," and won the 8th IEEE Communications Society (ComSoc) Asia–Pacific Outstanding Young Researcher Award in 2013. He was the recipient of nine Best (Student) Paper Awards from some reputable journals and conferences. He is the Winner of the 2016–2017 Excellence in Teaching Award, FCS, UNB. He currently serves as the Chair for IEEE ComSoc Communications and Information Security Technical Committee, and the Founding Co-Chair for IEEE TEMS Blockchain and Distributed Ledgers Technologies Technical Committee.

Qinyu Zhang (Senior Member, IEEE) received the bachelor's degree in communication engineering from Harbin Institute of Technology (HIT), Harbin, China, in 1994, and the Ph.D. degree in biomedical and electrical engineering from the University of Tokushima, Tokushima, Japan, in 2003.

From 1999 to 2003, he was an Assistant Professor with the University of Tokushima. He has been with HIT-Shenzhen (HITsz), Shenzhen, China, since 2003, and is currently a Full Professor and serves as the Vice President of HITsz. His research interests include aerospace communications and networks, and wireless communications and networks.

Prof. Zhang has been awarded the National Science Fund for Distinguished Young Scholars, the Young and Middle-Aged Leading Scientist of China, and the Chinese New Century Excellent Talents in University, and obtained three Scientific and Technological Awards from governments.